J Biomol NMR (2012) 54:343–353
DOI 10.1007/s10858-012-9676-8

ARTICLE

Spectral editing of two-dimensional magic-angle-spinning solid-state NMR spectra for protein resonance assignment and structure determination

K. Schmidt-Rohr · K. J. Fritzsching · S. Y. Liao · Mei Hong

Received: 17 August 2012 / Accepted: 14 September 2012 / Published online: 10 October 2012

Abstract Several techniques for spectral editing of 2D ^{13}C–^{13}C correlation NMR of proteins are introduced. They greatly reduce the spectral overlap for five common amino acid types, thus simplifying spectral assignment and conformational analysis. The carboxyl (COO) signals of glutamate and aspartate are selected by suppressing the overlapping amide N–CO peaks through ^{13}C–^{15}N dipolar dephasing. The sidechain methine (CH) signals of valine, lecuine, and isoleucine are separated from the overlapping methylene (CH_2) signals of long-chain amino acids using a multiple-quantum dipolar transfer technique. Both the COO and CH selection methods take advantage of improved dipolar dephasing by asymmetric rotational-echo double resonance (REDOR), where every other π-pulse is shifted from the center of a rotor period t_r by about 0.15 t_r. This asymmetry produces a deeper minimum in the REDOR dephasing curve and enables complete suppression of the undesired signals of immobile segments. Residual signals of mobile sidechains are positively identified by dynamics editing using recoupled ^{13}C–^{1}H dipolar dephasing. In all three experiments, the signals of carbons within a three-bond distance from the selected carbons are detected in the second spectral dimension via ^{13}C spin exchange. The efficiencies of these spectral editing techniques range from 60 % for the COO and dynamic selection experiments to 25 % for the CH selection experiment, and are demonstrated on well-characterized model proteins GB1 and ubiquitin.

K. Schmidt-Rohr · K. J. Fritzsching · S. Y. Liao · M. Hong (✉)
Department of Chemistry and Ames Laboratory,
Iowa State University, Ames, IA 50011, USA
e-mail: mhong@iastate.edu

Keywords Spectral editing · REDOR · CH selection · Protein secondary structure

Introduction

Recent progress in magic-angle-spinning (MAS) solid-state NMR (SSNMR) spectroscopy has made it possible to determine the three-dimensional structure of insoluble proteins such as membrane proteins (Hong et al. 2012; Luca et al. 2003) and amyloid fibrils (Tycko 2011). Central to this structure determination is the resolution of protein ^{13}C and ^{15}N peaks in multidimensional MAS correlation spectra and the assignment of these peaks to specific amino acid residues (Luca et al. 2003). Within the repertoire of multidimensional NMR correlation experiments for resonance assignment, the 2D ^{13}C–^{13}C correlation experiment based on ^{1}H-driven ^{13}C spin diffusion (PDSD) is especially widely used, since it is simple to perform and allows the assessment of protein homogeneity, sensitivity, and secondary structure. The 2D ^{13}C PDSD experiment is also the basis for distance extraction, since cross-peak intensities measured as a function of mixing time provide semi-quantitative distance information (Castellani et al. 2002).

While small proteins (<100 residues) with microcrystalline structural order can give completely resolved 2D PDSD spectra (Castellani et al. 2002; Franks et al. 2005a, b; Igumenova et al. 2004; Pauli et al. 2001), non-crystalline proteins usually exhibit ^{13}C linewidths of greater than 1 ppm (Su and Hong 2011). As a result, their 2D ^{13}C correlation spectra often show significant resonance overlap. While 3D and 4D experiments can be used to reduce resonance overlap, the high dimensionality severely reduces the sensitivity compared to 2D experiments; moreover, analyses of 3D and 4D spectra are much more time-consuming. For proteins

with linewidths exceeding 1 ppm, even 3D spectra often do not fully resolve all signals. Therefore, there are significant incentives to develop simple and efficient strategies to increase the information content of 2D NMR spectra and enable resonance assignment in the presence of line broadening.

Spectral editing has long been used to simplify and assign the SSNMR spectra of unlabeled organic compounds, whose sensitivity is too low for multidimensional ^{13}C correlation spectroscopy. 1D ^{13}C MAS spectra have been edited based on the number of attached protons per carbon (CH_n, n = 0, 1, 2) (De Vita and Frydman 2001; Frey and Opella 1984; Lesage et al. 1998; Mao and Schmidt-Rohr 2005; Sakellariou et al. 2001; Schmidt-Rohr and Mao 2002a, b; Wu et al. 1994; Wu and Zilm 1993), bonding to a heteronucleus such as nitrogen (Fang and Schmidt-Rohr 2009; Schmidt-Rohr and Mao 2002a, b), chemical shift anisotropy (Mao and Schmidt-Rohr 2004), and molecular motion, to give selective 1D ^{13}C spectra of different chemical functional groups. Based on spectral editing, the chemical composition of a variety of organic materials has been determined (Fang and Schmidt-Rohr 2009; Keeler and Maciel 2000; Mao et al. 2007a, b; Schmidt-Rohr et al. 2004). In comparison, spectral editing of 2D and 3D correlation spectra of ^{13}C, ^{15}N-enriched proteins has so far been restricted to the detection of the sidechain signals of several types of amino acids (Jehle et al. 2006a, b; Reggie et al. 2011). The potential for protein spectral editing is illustrated in Fig. 1: various amino acids with distinct functional groups exhibit similar chemical shifts. For instance, the ^{13}C chemical shifts of several methylene (CH_2) groups in Lys, Asp, and Arg are similar to the ^{13}C chemical shifts of the methine (CH) groups in Val, Leu and Ile, while backbone and sidechain carbonyl groups bonded to nitrogen share similar chemical shifts as the sidechain COO groups of Asp and Glu.

In this work, we demonstrate three spectral editing techniques that reduce such resonance overlap and facilitate assignment of 2D ^{13}C PDSD spectra of ^{13}C, ^{15}N-labeled proteins. First, ^{15}N–^{13}C dipolar dephasing is used to select the signals of the COO-containing Glu and Asp residues. Carboxyl sidechains are important in hydrogen bonding and ionic interactions such as those between proteins and biomineral surfaces (Goobes et al. 2006; Hoang et al. 2003). Despite their functional importance, an examination of the BMRB protein database shows that less than 5 % of Glu and Asp residues have assigned sidechain COO chemical shifts, indicating that standard multidimensional NMR techniques do not easily provide this information. Second, we select CH signals by suppressing the CH_2 signals using multiple-quantum recoupled dipolar dephasing (Mao and Schmidt-Rohr 2005). This method reveals the CH signals of Ile, Val, and Leu, which are found in fairly crowded but mutually exclusive regions of the 2D ^{13}C PDSD spectra. Third, we demonstrate the selection of mobile residues' signals by ^{13}C–^{1}H dipolar recoupled gated ^{1}H decoupling. Protein dynamics often contain important information about protein function (Hong 2006; Hong et al. 2012; Huster et al. 2001; Lorieau et al. 2008). While scalar-coupling based polarization transfer schemes can detect nearly isotropically mobile residues in proteins (Etzkorn et al. 2007), residues with anisotropic dynamics do not survive these solution-NMR-derived pulse sequences well, thus dipolar-based experiments to selectively detect dynamic residues are useful.

Common to these techniques is the novel use of asymmetrically positioned 180° pulses in the REDOR sequence (Gullion and Schaefer 1989), which enables complete dephasing of undesired signals. We demonstrate this asymmetric REDOR technique using numerical simulations and experiments. The spectral editing experiments presented here are tailored to MAS frequencies of ~10 kHz, which are higher than the typical MAS rates used for spectral editing of

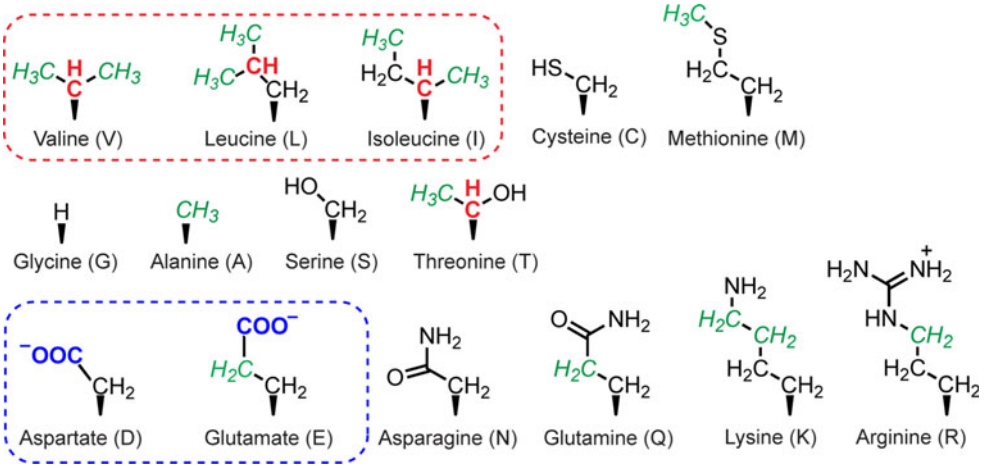

Fig. 1 Sidechain structures of aliphatic amino acid residues whose functional groups are spectrally edited here. *Red* Sidechain CH groups that are selected by the dipolar DEPT experiment. *Green italics* Dynamic groups that may be selected by the gated ^{1}H decoupling experiment. *Blue* Carboxyl groups that are selected by the ^{13}C–^{15}N REDOR experiment

unlabeled organic compounds (4–6 kHz), in order to better suppress ^{13}C–^{13}C dipolar couplings and obtain higher spectral resolution for ^{13}C-labeled proteins.

Experimental methods

Sample preparation

Uniformly ^{13}C, ^{15}N-labeled immunoglobulin-binding domain $\beta 1$ of the streptococcal protein G (GB1) was generously provided by Professor Chad Rienstra. Microcrystalline order was achieved by precipitating the protein using polyethylene glycol (PEG) (Franks et al. 2005a, b; Gallagher et al. 1994). The 56-residue GB1 has sufficient amino acid diversity for demonstrating COO, CH, and dynamics editing of the 2D spectra, and has excellent spectral resolution to enable complete resonance assignment. The sample was packed into a 2.5-mm MAS rotor by centrifugation. Bulk mother liquor was removed from the rotor by pipette. The protein was kept above 0 °C in all NMR experiments to avoid perturbation of the microcrystallinity by ice formation. Uniformly ^{13}C, ^{15}N-labeled ubiquitin in lyophilized powder form was obtained from Sigma-Aldrich and used without recrystallization.

Solid-state NMR experiments

SSNMR experiments on GB1 were carried out on a wide-bore Bruker AVANCE II-600 spectrometer (14.1 T) while ubiquitin spectra were measured on a wide-bore Bruker 400 MHz NMR spectrometer. 2.5-mm triple-resonance MAS probes were used and the samples were spun at a frequency of 10 kHz. Typical radio-frequency (rf) field strengths were 62.5 kHz for ^{13}C, 50 kHz for ^{15}N and 100 kHz for ^{1}H. ^{13}C chemical shifts were externally referenced to the carbonyl peak of α-Gly at 176.465 ppm, which is consistent with the adamantane CH_2 chemical shift of 38.48 ppm (Morcombe and Zilm 2003), both reported on the neat TMS scale. On this scale, the measured ^{13}C chemical shifts of GB1 are smaller by 2.4 ppm than the DSS-based values reported by Rienstra and coworkers (Franks et al. 2005a, b; Morcombe and Zilm 2003). This difference is verified to match most of the previously reported chemical shifts. The ^{1}H–^{13}C cross-polarization (CP) contact time was 1 ms. A ^{13}C spin diffusion mixing time of 20 ms was used to obtain primarily intra-residue cross peaks. ^{1}H irradiation at a field strength that matches the MAS frequency (DARR) was applied during the mixing time to facilitate ^{13}C spin diffusion (Takegoshi et al. 2001). For the ^{13}C–^{15}N REDOR period, ^{15}N inversion was achieved by composite $90°_{\phi-90}$ $180°_{\phi}90°_{\phi-90}$ pulses to reduce the effects of flip-angle errors (Sinha et al. 2004). ^{13}C, ^{15}N-enriched Gln, which contains both a COO and an N–CO group, was used to optimize the COO selection experiment. The main parameters of optimization to achieve complete suppression of the undesired peaks were the asymmetric timing of the ^{15}N π pulse within each rotor period in the COO selection experiment, the position and duration of the gated ^{1}H decoupling in the dynamic selection experiment, and the multiple-quantum (MQ) excitation time in the CH selection experiment.

Numerical simulations

REDOR curves were simulated using SPINEVOLUTION (Veshtort and Griffin 2006). ^{13}C and ^{15}N pulse lengths were finite and matched the values used in the experiments, which were 8 μs for ^{13}C and 10 μs for ^{15}N. Composite ^{15}N $90°_{\phi-90}$ $180°_{\phi}90°_{\phi-90}$ pulses were also used in the simulations. Where ^{1}H spins were included, 60–250 kHz continuous-wave decoupling was applied. The MAS rotation period was 100 μs, corresponding to the 10 kHz MAS frequency of the experiments. Asymmetric REDOR refocuses isotropic chemical shift as well as the chemical shift anisotropy, thus we ignored chemical shift in the simulations. Relaxation was also ignored. Powder averaging used a REPULSION scheme containing 700 sets of (α, β) angles for the crystallite orientations (Bak and Nielsen 1997).

Results and discussion

Principle of spectral editing by asymmetric REDOR

Figure 2 shows the pulse sequences of COO, CH, and dynamics edited 2D ^{13}C–^{13}C exchange experiments. In all three experiments, suppression of the undesired signals is achieved by recoupled heteronuclear dipolar interactions using a variant of REDOR (Gullion and Schaefer 1989), with two π-pulses per rotor period (t_r).

In spectral editing, it is crucial to dephase the undesired peaks, which are often larger than the signals of interest, to <2 %. The standard REDOR pulse sequence, where the π-pulses are spaced by $t_r/2$, generally does not permit this level of peak suppression. While the minimum of the ideal REDOR dephasing curve is −3 %, in practice the minimum is often raised to greater than 10 %, which precludes complete suppression of the undesired signals. The raised minimum can result from inaccurate flip angles of the recoupling pulses, whose effects are significantly but not completely suppressed by composite pulses (Sinha et al. 2004). A second cause is insufficient ^{1}H decoupling during the inversion pulses. Figure 3a displays the simulated REDOR dephasing curves for a 1.0-kHz dipolar coupling

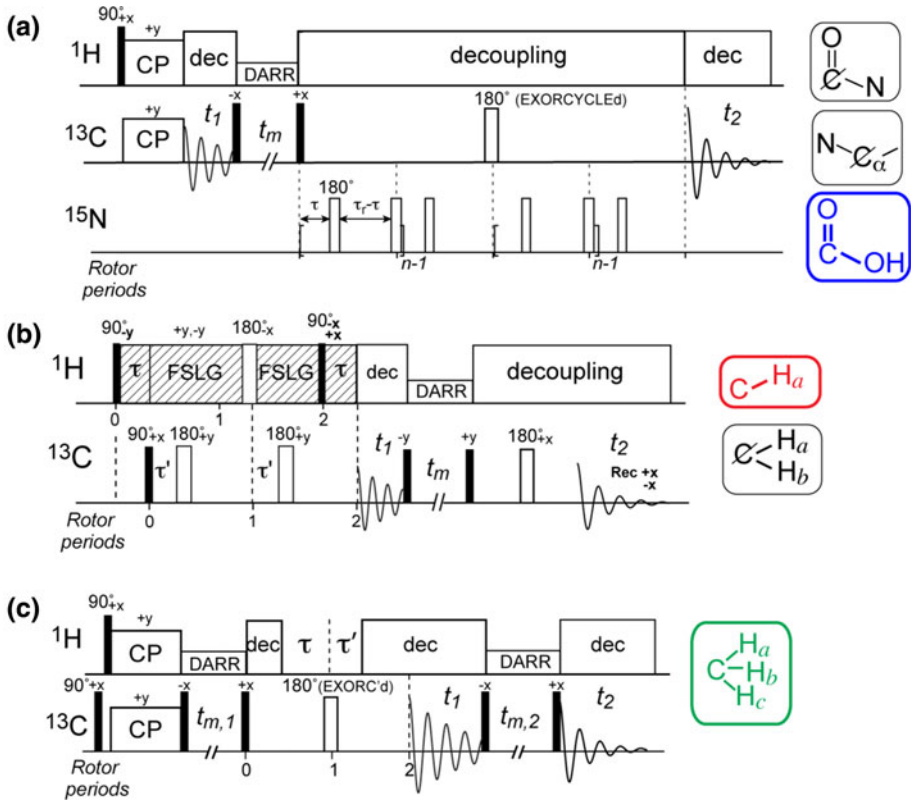

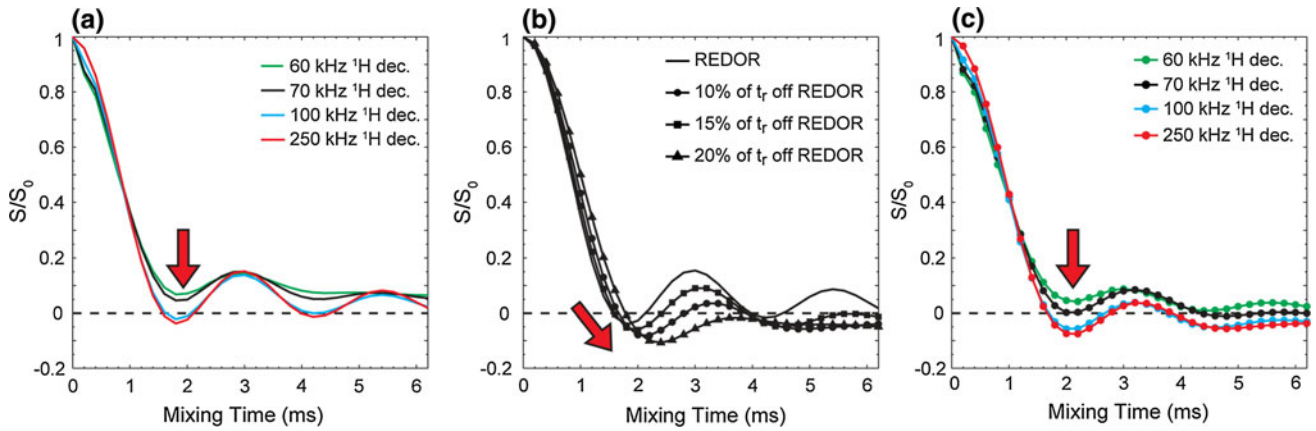

Fig. 2 Spectral editing pulse sequences for ^{13}C, ^{15}N-labeled proteins. **a** COO selection by ^{15}N–^{13}C asymmetric REDOR. **b** CH selection by dipolar DEPT. **c** Dynamic residue selection by ^{1}H–^{13}C recoupled gated decoupling. For (**a**) and (**c**), standard phase cycles involving inversion of the ^{1}H 90° excitation pulse with respect to spin lock, CYCLOPS of the ^{13}C pulses, and EXORCYCLE of the ^{13}C 180° pulse, are used, with corresponding changes of the receiver phase. For the DEPT experiment (**b**), the full phase cycle involves CYCLOPS permutation of the basic element shown here. All pulse programs can be found at http://www.public.iastate.edu/~nmrksr/

Fig. 3 Simulated ^{15}N–^{13}C REDOR dephasing curves for a 1.0-kHz ^{13}C–^{15}N dipolar coupling (corresponding to a ^{13}C–^{15}N distance of 1.458 Å) to achieve complete suppression of the ^{15}N-bonded ^{13}C signals. **a** Effects of ^{1}H decoupling field strength on regular symmetric REDOR dephasing. The weaker the ^{1}H decoupling field, the higher the minimum S/S_0. Zero crossing cannot be achieved at decoupling fields weaker than 70 kHz. A six-spin system containing one ^{13}C, one ^{15}N, and four protons was used, with a geometry that reflects the amino acid backbone plus two Hβ protons. **b** Effects of the π-pulse position within the rotor period on REDOR dephasing. Ideal ^{1}H decoupling is assumed by excluding protons in the simulations. The more asymmetric the π pulse position, the more negative the REDOR minimum, but at the expense of slowing down the REDOR oscillation. **c** Effects of ^{1}H decoupling field on the dephasing of 15 %-asymmetric REDOR. Zero crossing can be reached even under moderate ^{1}H decoupling. All simulations used composite ^{15}N π pulses with finite pulse lengths that are identical to the experimental pulse lengths

under moderate ^{1}H decoupling fields, where the minimum intensity is raised from the ideal value. For example, under 70-kHz ^{1}H decoupling, the REDOR minimum is +5 %. It has been shown empirically (Sinha et al. 2004) that the ratio of the ^{1}H and ^{15}N pulse field strengths must exceed three for the minimum of the REDOR curve to approach zero.

To lower the REDOR minimum to zero and completely suppress undesired signals at practical ^{1}H decoupling field strengths, we take advantage of asymmetric REDOR

(Gullion and Schaefer 1989). Here, the π pulses that are usually applied at the center of a rotor period are shifted by a fraction of t_r, typically 0.15 t_r (Fig. 2a). The effect of this asymmetry on the depth of the dephasing minimum can be understood qualitatively by considering the fact that the displacement of every other pulse moves the pulse sequence towards the quasi-static limit, where the smaller spacing between the recoupling pulses becomes so short that sample rotation during this period can be neglected (Bax et al. 1983; Tycko and Dabbagh 1990). The time signal of the spin-pair dipolar dephasing in the static limit is well known: it is the Fourier transform of the Pake pattern, and has the desired deep minimum below zero due to the oscillation associated with the doublet peaks of the Pake pattern (Schmidt-Rohr and Spiess 1994).

For a quantitative analysis, Fig. 3b shows simulated REDOR dephasing curves under ideal ^{1}H decoupling for varying positions of the π pulse, specified in terms of the fraction of t_r by which the pulse within the rotor period is shifted from the center of each rotor period. With 10–20 % asymmetry, the REDOR minimum ranges from -6 to -11 %, thus establishing zero-crossing points for complete suppression of the undesired signals. The secondary maxima, which have significant intensities in standard REDOR, also decrease in intensity, and the time regime with low intensities broaden, both facilitating peak suppression. When a ^{1}H decoupling field of realistic strength is applied, the asymmetric-REDOR dephasing curves retain the downward shift of the minimum intensity (Fig. 3c). For example, under 70 kHz ^{1}H decoupling, the intensity of the first minimum is zero for a pulse shift of 10–15 % t_r, compared to the minimum intensity of +5 % when standard symmetric REDOR is used.

COO selection by N–CO suppression

Figure 4 demonstrates COO selection of 2D ^{13}C PDSD spectra by asymmetric ^{13}C–^{15}N REDOR. We used 15 % asymmetry and a total REDOR period of 2.2 ms to completely suppress the peaks of immobile N–CO and N–Cα carbons. The REDOR period can be placed either before the t_1 period to suppress the C–N signals in the ω_1 dimension (Fig. 4b) or between the t_1 and t_2 periods to suppress the signals in the ω_2 dimension (Fig. 4c). Since the 2D ^{13}C PDSD spectrum usually shows higher cross peak intensities on the upper left side ($\omega_1 < \omega_2$) than the lower right side ($\omega_1 > \omega_2$) of the diagonal due to the higher CP efficiency of protonated carbons, we focus on the ω_2-edited CN-free spectrum.

Figure 5 shows the expanded carbonyl-aliphatic region of the full versus ω_2-COO-selected 2D spectra. In the full spectrum (Fig. 5a), the cross peaks of Asp and Glu COO groups partially overlap with the NCO peaks of Asn and Gln sidechains, and the COO–Cα cross peaks of Glu and Asp partially overlap with the Ala CO–Cα cross peaks. With a 2.2-ms ^{13}C–^{15}N REDOR dephasing time, all cross peaks to the backbone NCO and most of the sidechain Asn and Gln signals are suppressed, while all cross peaks of Asp and Glu

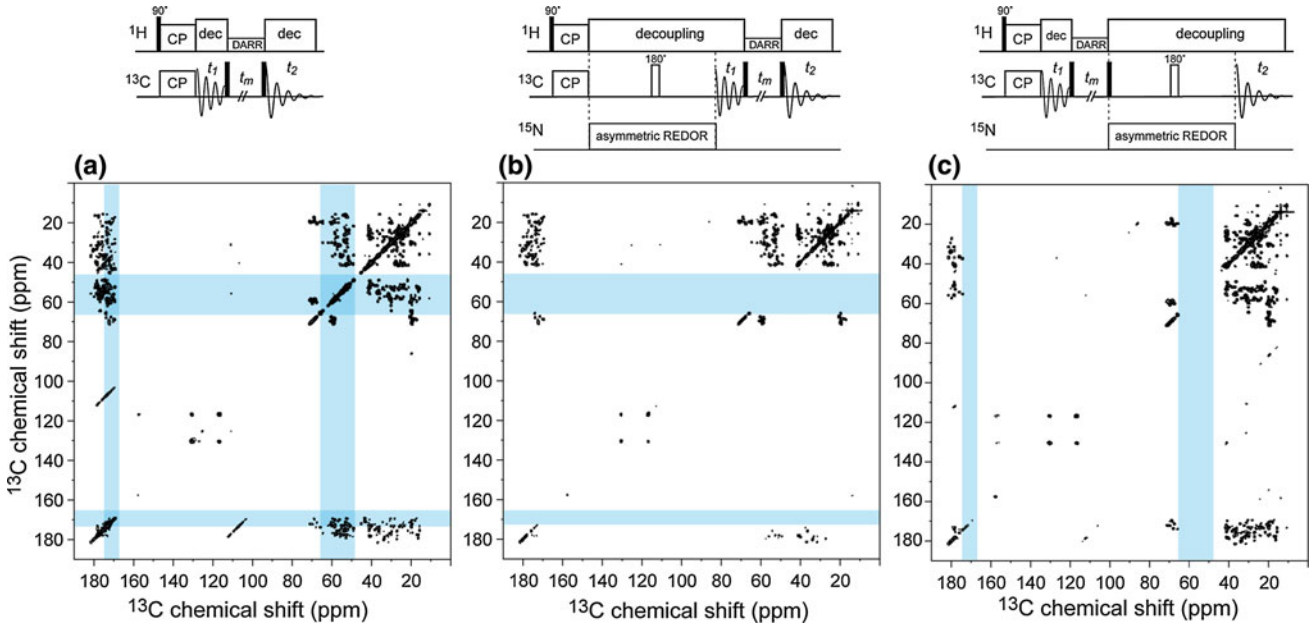

Fig. 4 COO selection of the 2D ^{13}C–^{13}C correlation spectra by ^{15}N–^{13}C dipolar dephasing. **a** Unedited 2D PDSD spectrum of GB1. **b** ω_1-edited 2D spectrum, where the Cα and N–CO signals are removed in the ω_1 dimension. **c** ω_2-edited 2D spectrum, where the Cα and N–CO signals are suppressed in the ω_2 dimension. The pulse sequence for each spectrum is shown at the top to clarify the distinction between the ω_1 and ω_2-edited spectra. *Shaded blue bars* indicate the region where N–Cα and N–CO signals are suppressed

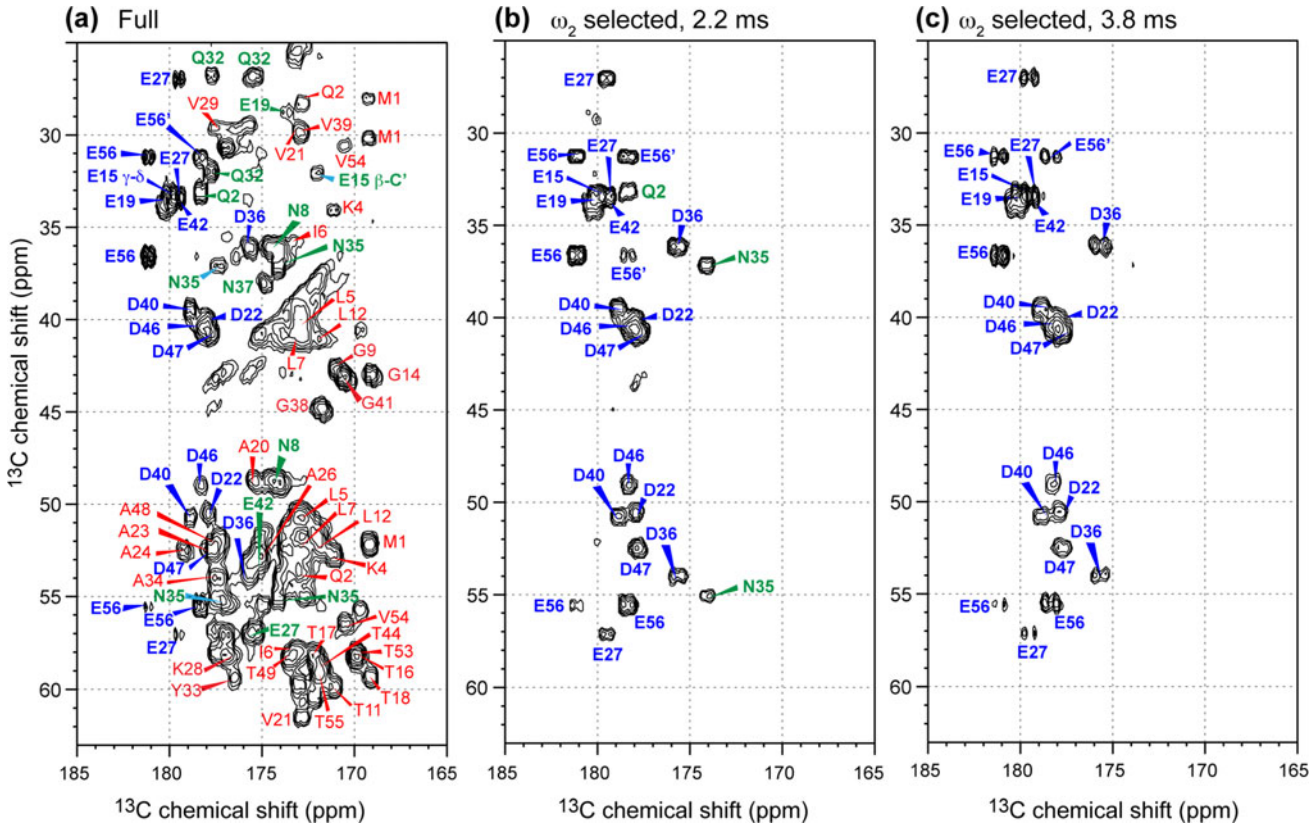

Fig. 5 Expanded carbonyl region of the 2D COO-selected spectra. **a** Unfiltered spectrum. The COO signals of Glu (E) and Asp (D) are assigned in *blue*, the sidechain and backbone N–CO signals of Gln (Q) and Asn (N) are assigned in *green*, and the backbone N–CO signals of all other amino acids are assigned in *red*. The backbone COO peaks of the terminal E56 are denoted as E56′. **b** ω_2-COO selected spectrum with a REDOR period of 2.2 ms. **c** ω_2-COO-selected spectrum with a REDOR period of 3.8 ms. The signals of dynamic Q2 and N35 (*green*), which survive the 2.2 ms filter, are suppressed by the longer REDOR time. Spectra (**b**, **c**) were measured with $\tau = 40$ μs in Fig. 2a, which shifts the position of the ^{15}N π pulse within the rotor period by $0.1t_r$ before the center of the rotor period

sidechain COO and the signal of the terminal COO of the protein backbone (E56) survive (Fig. 5b). The only signals that should not be present are those of N35 and Q2 sidechains; presumably they remain due to partial motional averaging of the ^{13}C–^{15}N dipolar coupling. Using a longer REDOR dephasing time of 3.8 ms, we were able to suppress these signals (Fig. 5c) while retaining the Glu and Asp peaks, giving a cleanly edited COO-only spectrum.

The 2D PDSD spectra were measured using a spin diffusion mixing time of 20 ms, which allowed the observation of intra-residue cross peaks within two or three bonds from the COO carbons. The peak positions of Asp (D) are mostly in a rectangle between 175 and 179 ppm in the ω_2 dimension and 35 and 55 ppm in the ω_1 dimension. These signals are relatively distinct from the Glu (E) peaks, which have larger COO (ω_2) frequencies and thus appear more to the left. Thus, type assignment of Glu and Asp residues can be made based on the peak positions in the COO-selected 2D spectra.

The frequencies of the Cβ and Cα peaks in each vertical slice of the ω_2-COO-selected spectrum contain valuable information about the secondary structure of the Glu and Asp residues. For instance, the peak positions for D36, with a relatively small Cβ and relatively large Cα chemical shift, are characteristic of an α-helix (Wishart et al. 1992). The same is true for E27, which exhibits peaks at the top and bottom of the spectrum. On the other hand, the chemical shifts of D46 suggest a β-sheet conformation. These conclusions are in agreement with the structure of GB1 and were previously obtained from 3D NMR analysis (Franks et al. 2008). We point them out here to demonstrate how spectrally edited 2D spectra can provide a low-resolution view of the protein secondary structure, in a manner that would be compatible with significant line broadening. Since the COO-selected 2D spectrum is sparse, longer spin diffusion mixing times can be used to detect inter-residue contacts from the Glu and Asp sidechains to provide valuable tertiary structure constraints.

The sensitivity of this COO selection experiment is very high, about 60 % of the unedited experiment. The intensity reduction mainly results from ^{13}C T_2 relaxation and evolution under ^{13}C–^{13}C J-coupling during the REDOR mixing period.

CH and dynamic selection experiments

To select the CH signals in 2D spectra, we used the dipolar analog of the DEPT (distortionless enhancement by polarization transfer) experiment, adapted for 10-kHz MAS (Fig. 2b) (Schmidt-Rohr and Mao 2002a, b). In this experiment, ^{1}H magnetization H_x is converted to two-spin coherence C_zH_y by a short evolution period (τ) under C–H dipolar coupling. A 90° x-pulse on ^{13}C converts this coherence to C_yH_y, a combination of double- and zero-quantum coherence. For methine (CH) groups, this two-spin coherence survives the subsequent dephasing period with heteronuclear C–H dipolar recoupling, since it commutes with the heteronuclear dipolar Hamiltonian $\omega_{CH}2C_zH_z$, while the additional proton in CH_2 groups destroys this coherence by its dipolar coupling to the carbon. Using a ^{1}H 90° x-pulse and a second heteronuclear evolution period τ identical to the first, the surviving two-spin coherence of CH groups is reconverted to observable ^{13}C magnetization $-C_x$. Thus, the MQ excitation and reconversion period, in addition to removing the CH_2 signals, also serves to transfer polarization from ^{1}H to ^{13}C.

During the excitation, evolution, and reconversion of the MQ coherence, ^{1}H–^{1}H homonuclear dipolar couplings are suppressed by the FSLG sequence (Bielecki et al. 1989). Because of the dependence of the dipolar couplings on the rotor orientation, the MQ reconversion period and excitation period must be separated by an integer multiple of t_r, except when the excitation period is half a t_r, in which case the two periods can be separated by multiples of $t_r/2$. The ^{1}H and ^{13}C π pulses during the MQ evolution period between the ^{13}C 90° pulse and the second ^{1}H 90° pulse prevent the refocusing of the heteronuclear dipolar evolution by MAS. In addition, they refocus most of the ^{1}H and all of the ^{13}C chemical shift evolution. The π pulses are spaced in the asymmetric REDOR fashion, with a shift of every other pulse by $\sim$20 % of t_r.

Figure 6a, b compares the full 2D PDSD spectrum with the CH-edited spectrum, in which the CH signals of Val, Leu and Ile (in red) are selected and resolved from the overlapping CH_2 resonances. The selection particularly allowed the identification of the Val Cβ–Cα cross peaks, which overlap significantly with the Lys, Glu and Gln cross peaks. Leu Cγ–Cβ cross peaks also benefitted from editing and became resolved from various Lys peaks. The CH signals of these three amino acids fall into three bands with little overlap (34–28 ppm from TMS for Val, 26–23 ppm for Leu, and 42–32 ppm for Ile), showing highly characteristic cross-peak patterns. Thus, the CH selection allows amino acid type assignment simply from the observed peak positions in most cases. The sensitivity of the CH-edited spectrum is about 25 % of the full spectrum. This is comparable to the sensitivity of most homonuclear double-quantum filtered 2D experiments and heteronuclear 3D NCC experiments.

As before for Glu and Asp, the resolved Cα and Cβ chemical shifts of Val, Leu and Ile from the edited 2D spectrum provide information on the backbone conformation. For instance, V29 with its high Cα and low Cβ shifts is clearly in an α-helix, while V54 at the other end of the Cα chemical shift range is expected to be in a β-sheet. The chemical shifts of I6 show that it is clearly not in an α-helix, but suggest a β-sheet. None of the three Leu residues in the protein (L5, L7, and L12) show α-helical characteristics, indicating that the α-helix does not include residues 5 through 12. These conclusions are consistent with the previous 3D NMR analysis (Franks et al. 2005b).

The CH edited spectrum in Fig. 6b also retains undesired signals of mobile CH_2 groups (in green italics) of some long aliphatic sidechains, in particular Lys residues. These signals of dynamic residues could be reduced significantly by using a short MQ excitation and reconversion time of $\sim$30 µs. Fortunately, there is no significant spin exchange from sites far out in mobile sidechains to backbone Cα or CO. Therefore, the Cα–Cβ or Cα–Cγ cross peaks of Ile, Val, and Leu can be determined unambiguously. In addition, the cross peaks of Lys Cε and Cδ are mostly resolved from the CH-selected Cβ–Cγ signals of Ile and Val. Alternatively, CH selection at low temperature where motion is suppressed can remove the CH_2 signals. Scalar-coupling based spectral editing may also provide an alternative approach to select CH signals independent of motion (Sakellariou et al. 2001).

When studying proteins at physiological temperature, one can identify the dynamic residues using a dynamics selection experiment (Fig. 2c). In this experiment, a 60-µs period without ^{1}H decoupling is combined with a ^{13}C π pulse that recouples the ^{1}H–^{13}C dipolar interaction. The polarization of the dynamic moieties was enhanced by combining direct polarization and cross polarization, with a 90° ^{13}C pulse before CP. After CP, a 90° pulse flips the ^{13}C magnetization to the z-direction and a $\sim$50 ms mixing period was applied to transfer the magnetization from the well-polarized rigid protonated carbons to the mobile segments and the non-protonated carbons. This combined polarization approach is general and can be incorporated whenever the signals of both mobile and rigid residues are of interest. It complements scalar-coupling based polarization transfer schemes that detect only residues with nearly isotropic mobility in proteins (Etzkorn et al. 2007).

Figure 6c shows the dynamics edited spectrum, where the signals of all methyl groups and the methylene signals of several Lys and Glu residues are detected. The spectrum indicates which peaks in the CH-selected spectrum result from mobile CH_2 and CH_3 groups. The efficiency is about 50 % for methyl groups and highly mobile methylene groups.

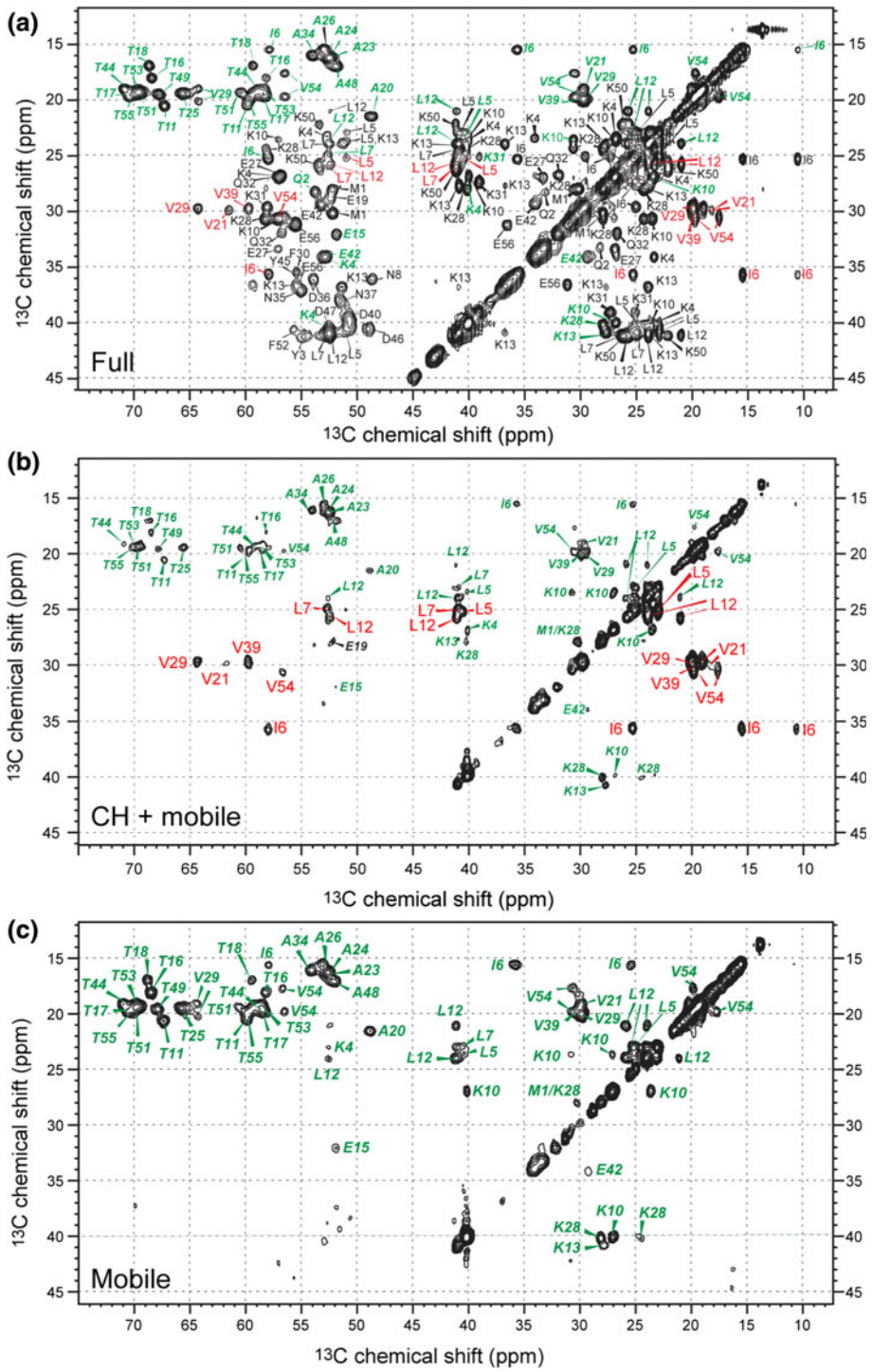

Fig. 6 CH and dynamics editing of the 2D PDSD spectrum of GB1. **a** Aliphatic region of the unedited spectrum. The CH signals are assigned in *red* and the dynamic signals are assigned in *green italic*. **b** CH-selected 2D spectrum, showing the suppression of immobile CH_2 signals in the ω_1 dimension. Residual non-CH signals result from the methyl groups and dynamic CH_2 moieties. **c** Dynamics selected 2D spectrum, measured using gated ^{1}H decoupling with $\tau = 40$ μs and $\tau' = 20$ μs. The ^{13}C spin diffusion mixing time was 20 ms for all spectra

Mobile segments

The dynamics edited 2D spectrum of Fig. 6c shows that the ends of several Lys sidechains (K10, K13, and K28) undergo large-amplitude motions, while others (K31 and K50) do not move significantly. The behavior of K4 is difficult to assess, since its Cγ–Cε chemical shifts nearly coincide with those of K10. The chemical shifts of Cγ and Cδ of K28 were interchanged relative to Table 1 in (Franks et al. 2005a, b) to match the observed cross peaks in Fig. 6a, c.

The Lys Cε–Cδ cross-peak intensities suggest that the motional amplitude decreases from K10 through K28 to K13. K10 is so mobile that its signal is suppressed by the short C–H MQ excitation period used to obtain the spectrum in Fig. 6b. The dynamics edited spectrum of Fig. 6c

most prominently exhibits the various cross peaks of K10, which is uniquely identified based on its Cβ chemical shift. These peaks indicate that not only Cε but also Cδ and Cγ of K10 undergo large-amplitude motion. This is consistent with the position of K10 in the loop between the β_1 and β_2 strands (Franks et al. 2008). The lack of mobility of K31 may be attributed to its position in the central α-helix, but the absence of dynamics for K50 is somewhat surprising, since K50 is located in the loop between the β_4 and β_5 strands (Franks et al. 2008).

The dynamics of the M1 and Q2 sidechains may be attributed to increased mobility near the N terminus of the protein. In Fig. 6b, we observe a relatively weak Cβ–Cα cross peak of V21, located in the loop between the β_2 and β_3 strands, which is also due to dynamics as discussed in (Franks et al. 2008).

Application of spectral editing to disordered proteins with broad lines

To demonstrate how spectral editing can facilitate secondary structure analysis of disordered proteins with broad linewidths, we measured the 2D ^{13}C PDSD spectra of uniformly ^{13}C-labeled ubiquitin. The sample is a lyophilized powder that was not subject to crystallization and thus exhibits ^{13}C linewidths of 1–2 ppm. The ^{13}C chemical shifts of microcrystalline ubiquitin have been almost fully assigned (Igumenova et al. 2004), thus allowing us to verify our conclusions.

Figure 7 shows the full (a) and CH-selected (b) 2D spectra: the cross peak patterns are significantly simplified after CH selection. The selected signals of the seven Ile, four Val, and eight Leu residues in ubiquitin can be analyzed in terms of β-sheet, α-helix, and loop conformations. All three amino-acid types show strong Cα/Cβ cross peaks for multiple residues at positions typical of β-sheet (e.g., Ile: 58/39 ppm, TMS scale; Val: 57/34 ppm). Much smaller peaks of one or two residues each are observed at positions characteristic of α-helices (Ile: 64/34 ppm, Val: 65/28 ppm). Various Cβ–Cγ cross peaks of Ile were observed around a Cβ chemical shift of 33 ppm, which is typically associated with the α-helical conformation, but not all these have Cα chemical shifts typical of α-helices. This suggests Ile in a loop or at the end of an α-helix, which is confirmed by a distinct Cβ–Cδ cross peak (marked 'loop') with an unusually low Cβ but also a low Cα chemical shift, incompatible with α-helix or β-sheet. On the basis of these cross peak positions, one can propose that the protein is significantly β-sheet but also contains some α-helical segments and loops; indeed, ubiquitin has ~35 % β-sheet and ~25 % α-helical residues (Heinig and Frishman 2004; Kabsch and Sander 1983).

This type of secondary-structure information can often be gleaned from the resolved Cα–Cβ cross peaks of Ala,

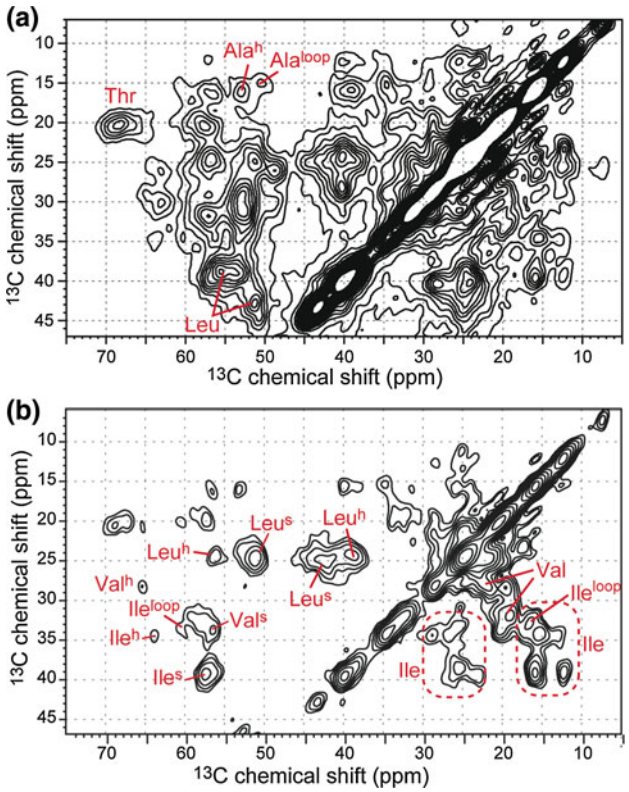

Fig. 7 2D ^{13}C PDSD spectra of lyophilized ubiquitin **a** without editing and **b** with CH selection. The CH selection is applied to the ω_1 dimension of the 2D spectrum. Amino acid types are annotated along with the identified secondary structures. Helix: h; sheet: s, and loop. The spectra were measured at room temperature on a 400 MHz SSNMR spectrometer

but the two Ala residues in ubiquitin show no β-sheet character, only an α-helical and a loop conformation (Fig. 7a). Only in some of the Thr Cα–Cβ peaks far off the diagonal (not shown) does the unedited spectrum give a clear indication of a high β-sheet content.

Next, one can look for segments in the amino acid sequence of ubiquitin containing one Ala, Ile, Val, and Leu residue each, as candidates for α-helical stretches. This search yielded the segment Val26–Ile30 (VKAKI), which is indeed part of an α-helix in ubiquitin, as well as Leu43–Ala46 (LIFA), which is not α-helical (Igumenova et al. 2004). To distinguish between these two cases, sequential resonance assignment is necessary.

In summary, the CH-selected 2D spectrum yields secondary-structure information and helps with the identification of secondary-structure elements even in the presence of significant line broadening.

Potential spectral editing in 3D NMR

The COO selection experiment can be incorporated into 3D NCOCX and NCACX experiments, to permit assignment

of residues close to Asp and Glu, with minimum resonance assignment. The pulse sequence module should be implemented in the ω_3 ^{13}C dimension, to remove non-E/D signals. The dynamics editing experiment can also be incorporated into 3D NCC experiments, provided that long mixing times are used to transfer the backbone CO or Cα magnetization to the mobile sidechain ends.

Acknowledgments We thank Professor Chad Rienstra for providing the microcrystalline ^{13}C, ^{15}N-labeled GB1 and Tuo Wang for help with the experiments. This work was supported by the National Institutes of Health grant GM088204 (M. H., K.J. F and S.Y. L.) for the 600 MHz NMR experiments and by the U.S. Department of Energy, Office of Basic Energy Sciences, Division of Materials Sciences and Engineering under Award AL-90-360-001 (to K.S-R) for the 400 MHz NMR experiments.

References

Bak M, Nielsen NC (1997) REPULSION, a novel approach to efficient powder averaging in solid-state NMR. J Magn Reson 125:132–139

Bax A, Szeverenyi NM, Maciel GE (1983) Chemical shift anisotropy in powdered solids studied by 2D Fourier transform NMR with flipping of the spinning axis. J Magn Reson 55:494–497

Bielecki A, Kolbert AC, Levitt MH (1989) Frequency-switched pulse sequences: homonuclear decoupling and dilute spin NMR in solids. Chem Phys Lett 155:341–346

Castellani F, vanRossum B, Diehl A, Schubert M, Rehbein K, Oschkinat H (2002) Structure of a protein determined by solid-state magic-angle spinning NMR spectroscopy. Nature 420:98–102

De Vita E, Frydman L (2001) Spectral editing in (13)C MAS NMR under moderately fast spinning conditions. J Magn Reson 148: 327–337

Etzkorn M, Martell S, Andronesi OC, Seidel K, Engelhard M, Baldus M (2007) Secondary structure, dynamics, and topology of a seven-helix receptor in native membranes, studied by solid-state NMR spectroscopy. Angew Chem Int Ed Engl 46:459–462

Fang XW, Schmidt-Rohr K (2009) Fate of the amino acid in glucose-glycine melanoidins investigated by solid-state nuclear magnetic resonance. J Agric Food Chem 57:10701–10711

Franks WT, Zhou DH, Wylie BJ, Money BG, Graesser DT, Frericks HL, Sahota G, Rienstra CM (2005a) Dipole tensor-based atomic-resolution structure determination of a nanocrystalline protein by solid-state NMR. J Am Chem Soc 127:12291–12305

Franks WT, Zhou DH, Wylie BJ, Money BG, Graesser DT, Frericks HL, Sahota G, Rienstra CM (2005b) Magic-angle spinning solid-state NMR spectroscopy of the beta1 immunoglobulin binding domain of protein G (GB1): 15N and 13C chemical shift assignments and conformational analysis. J Am Chem Soc 127:12291–12305

Franks WT, Wylie BJ, Schmidt HL, Nieuwkoop AJ, Mayrhofer RM, Shah GJ, Graesser DT, Rienstra CM (2008) Magic-angle spinning solid-state NMR spectroscopy of the β1 immunoglobulin binding domain of protein G (GB1): 15N and 13C chemical shift assignments and conformational analysis. Proc Natl Acad Sci USA 105:4621–4626

Frey MH, Opella SJ (1984) 13C spin exchange in amino acids and peptides. J Am Chem Soc 106:4942–4945

Gallagher T, Alexander P, Bryan P, Gilliland GL (1994) Two crystal structures of the B1 immunoglobulin-binding domain of streptococcal protein G and comparison with NMR. Biochemistry 33:4721–4729

Goobes G, Goobes R, Schueler-Furman O, Baker D, Stayton PS, Drobny GP (2006) Folding of the C-terminal bacterial binding domain in statherin upon adsorption onto hydroxyapatite crystals. Proc Natl Acad Sci USA 103:16083–16088

Gullion T, Schaefer J (1989) Rotational echo double resonance NMR. J Magn Reson 81:196–200

Heinig M, Frishman D (2004) STRIDE: a web server for secondary structure assignment from known atomic coordinates of proteins. Nucleic Acids Res 32, Web Server Issue

Hoang QQ, Sicheri F, Howard AJ, Yang DSC (2003) Bone recognition mechanism of porcine osteocalcin from crystal structure. Nature 425:977–980

Hong M (2006) Oligomeric structure, dynamics, and orientation of membrane proteins from solid-state NMR. Structure 14:1731–1740

Hong M, Zhang Y, Hu F (2012) Membrane protein structure and dynamics from NMR spectroscopy. Annu Rev Phys Chem 63: 1–24

Huster D, Xiao LS, Hong M (2001) Solid-state NMR investigation of the dynamics of colicin Ia channel-forming domain. Biochemistry 40:7662–7674

Igumenova TI, McDermott AE, Zilm KW, Martin RW, Paulson EK, Wand AJ (2004) Assignments of carbon NMR resonances for microcrystalline ubiquitin. J Am Chem Soc 126:6720–6727

Jehle S, Hiller M, Rehbein K, Diehl A, Oschkinat H, van Rossum BJ (2006a) Spectral editing: selection of methyl groups in multidimensional solid-state magic-angle spinning NMR. J Biomol NMR 36:169–177

Jehle S, Rehbein K, Diehl A, van Rossum BJ (2006b) Amino-acid selective experiments on uniformly 13C and 15N labeled proteins by MAS NMR: filtering of lysines and arginines. J Magn Reson 183:324–328

Kabsch W, Sander C (1983) Dictionary of protein secondary structure: pattern recognition of hydrogen-bonded and geometrical features. Biopolymers 22:2577–2637

Keeler C, Maciel GE (2000) ^{13}C NMR spectral editing of humic material. J Mol Struct 550–551:297–305

Lesage A, Steuernagel S, Emsley L (1998) Carbon-13 spectral editing in solid-state NMR using heteronuclear scalar couplings. J Am Chem Soc 120:7095–7100

Lorieau JL, Day LA, McDermott AE (2008) Conformational dynamics of an intact virus: order parameters for the coat protein of Pf1 bacteriophage. Proc Natl Acad Sci USA 105:10366–10371

Luca S, Heise H, Baldus M (2003) High-resolution solid-state NMR applied to polypeptides and membrane proteins. Acc Chem Res 36:858–865

Mao JD, Schmidt-Rohr K (2004) Separation of aromatic-carbon C-13 NMR signals from di-oxygenated alkyl bands by a chemical-shift-anisotropy filter. Solid State Nucl Magn Reson 26:36–45

Mao J-D, Schmidt-Rohr K (2005) Methylene spectral editing in solid-state 13C NMR by three-spin coherence selection. J Magn Reson 176:1–6

Mao J-D, Cory RM, McKnight DM, Schmidt-Rohr K (2007a) Characterization of a nitrogen-rich fulvic acid and its precursor algae by solid-state NMR. Org Geochem 38:1277–1292

Mao J-D, Tremblay L, Gagné J-P, Kohl S, Rice J, Schmidt-Rohr K (2007b) Natural organic matter in the Saguenay Fjord and the St. Lawrence Estuary investigated by advanced solid-state NMR. Geochim Cosmochim Acta 71:5483–5499

Morcombe CR, Zilm KW (2003) Chemical shift referencing in MAS solid state NMR. J Magn Reson 162:479–486

Pauli J, Baldus M, vanRossum B, Groot Hd, Oschkinat H (2001) Backbone and side-chain 13C and 15N signal assignments of the alpha-spectrin SH3 domain by magic-angle spinning solid-state NMR at 17.6 Tesla. ChemBioChem 2:272–281

Reggie L, Lopez JJ, Collinson I, Glaubitz C, Lorch M (2011) Dynamic nuclear polarization-enhanced solid-state NMR of a

13C-labeled signal peptide bound to lipid-reconstituted Sec translocon. J Am Chem Soc 133:19084–19086
Sakellariou D, Lesage A, Emsley L (2001) Spectral editing in solid-state NMR using scalar multiple quantum filters. J Magn Reson 151:40–47
Schmidt-Rohr K, Mao J-D (2002a) Selective observation of nitrogen-bonded carbons in solid-state NMR by saturation-pulse induced dipolar exchange with recoupling. Chem Phys Lett 359:403–411
Schmidt-Rohr K, Mao JD (2002b) Efficient CH-group selection and identification in C-13 solid-state NMR by dipolar DEPT and H-1 chemical-shift filtering. J Am Chem Soc 124:13938–13948
Schmidt-Rohr K, Spiess I HW (1994) Multidimensional solid-state NMR and polymers. Academic Press, San Diego
Schmidt-Rohr K, Mao JD, Olk DC (2004) Nitrogen-bonded aromatics in soil organic matter and their implications for a yield decline in intensive rice cropping. Proc Natl Acad Sci USA 101:6351–6354
Sinha N, Schmidt-Rohr K, Hong H (2004) Compensation for pulse imperfections in rotational-echo double-resonance NMR by composite pulses and EXORCYCLE. J Magn Reson 168:358–365
Su Y, Hong M (2011) Conformational disorder of membrane peptides investigated from solid-state NMR linewidths and lineshapes. J Phys Chem B 115:10758–10767
Takegoshi K, Nakamura S, Terao T (2001) C-13-H-1 dipolar-assisted rotational resonance in magic-angle spinning NMR. Chem Phys Lett 344:631–637
Tycko R (2011) Solid-state NMR studies of amyloid fibril structure. Annu Rev Phys Chem 62:279–299
Tycko R, Dabbagh G (1990) Measurement of nuclear magnetic dipole-dipole couplings in magic angle spinning NMR. Chem Phys Lett 173:461–465
Veshtort M, Griffin RG (2006) SPINEVOLUTION: a powerful tool for the simulation of solid and liquid state NMR experiments. J Magn Reson 178:248–282
Wishart DS, Sykes BD, Richards FM (1992) The chemical shift index: a fast and simple method for the assignment of protein secondary structure through NMR spectroscopy. Biochemistry 31:1647–1651
Wu XL, Zilm KW (1993) Spectral editing in CPMAS NMR. Generating subspectra based on proton multiplicities. J Magn Reson A 102:205–213
Wu X-L, Burns ST, Zilm KW (1994) Complete spectral editing in CPMAS NMR. J Magn Reson A 111:29–36